CHAPTER II

LITERATURE REVIEWS

2.1 Multiscale molecular simulations of two polymer hosts for gel electrolytes: poly(vinyl chloride) and poly(vinyl fluoride)

Polymer electrolytes are an attractive option to substitute liquid solutions due to their thermal stability and high flexibility (Daniel, 2013). Polymer electrolytes can be divided into two groups: solid and gel electrolytes. Solid polymer electrolytes (SPEs) are electrolytes in which alkali salts can be dissolved in the appropriate polymers. The host polymers play a role in the diffusion of alkali ions through the local movement of chain segments. The first SPE was reported in the 1970s using poly (ethylene oxide), PEO (Fenton, 1973; Wright, 1975). For ionic conductivity in alkali metal-PEO complexes, it has been proposed that metal ions work as charge carriers in the non-crystalline phase of the polymer host. Ionic diffusion occurs through the formation and dissociation of the coordination structure between cations and oxygen atoms in PEO (Ratner, 1988). The disadvantage of PEO is a very low metal ion transportation caused by the crystallization and trapping effects due to the strong coordination between the PEO backbone and metal ions (Capiglia, 1999; Zhang, 2014; Itoh, 2017).

Compared to SPEs, gel polymer electrolytes (GPEs) have higher ionic conductivity with good interfacial and mechanical properties due to the liquid phase and solid component. The electrolyte in the liquid state is immobilized in the polymeric matrix and forms the gel phase. GPEs could combine advantages from both liquid and solid components. GPEs can be found in the form of either the heterogeneous (phase-separated) or the homogeneous (uniform) gel. Heterogeneous GPEs are composed of a polymer network with interconnected pores filled with liquid electrolytes.

The metal ions in heterogeneous GPEs can diffuse in the swollen-gelled phase. Most of GPEs exhibit higher ionic conductivity in the order of 10^{-3} Scm^{-1} at room temperature. Consequently, GPEs are one of the potential polymer electrolytes for the battery application with enhanced efficiency and safety.

2.1.1 Rotational isomeric state (RIS) model of PVC

The mean-square unperturbed dimensions of vinyl polymers frequently a dependent on strongly on stereochemical composition, as noted in the innumerable instances mention in the book on the rotational isomeric state model (Flory, 1969; Mattice, 1994; Rehahn, 1997). The unperturbed dimensions have usually been calculated as a function of P_m, the probability for a meso (m) diad, using the presupposition of Bernoullian statistics. This method brings averaging of the mean-square unperturbed dimensions through various chains many different at each p_m, $0 < p_m < 1$, to take into account sufficient randomness of the stereochemical sequence.

The construction of metal catalysts allows for better control over the stereochemical sequence of vinyl polymers. This handle can consist the installation of a stereochemically pure isotactic and syndiotactic polymers, in which the only *diads* are *m* or *racemo* (*r*), respectively. It might likewise consist forced synthesis of chains in which the primary duplicate for the stereochemical series expand an array prolonged than a single diad, e.g., *mr*, *mmr*, etc. This potential ability in synthesis forces curiosity in conjectured behaviour of chains in which the stereochemical orders consist of reiterations of a small thread of diads. This attention will help to identify the sequence that tends to provide the newest features and to explicate an understanding of the origination of tendencies in family effects chains with methodically related repeat units.

Poly(vinyl chloride) is a renowned atactic polymer. For decades, stereochemical compositions have been dealt with in a limited range by performing the polymerization at different temperatures. Bovey reports that pm can vary from 0.37 (for polymerization at -78 °C) to 0.46 (for polymerization at 100 °C) (Bovey, 1967). Most of the commercial materials are in this range. Pay attention to the use of vinyl chloride in the preparation of polymers with different properties from those of the usual *atactic* material, it's worth it to question which repeating stereochemical series,

apart from that of the pure isotactic and pure syndiotactic polymer, could perform variously than before atactic structure. An uncomplicated consideration for each a series is to calculate the mean square dimension for conventional atactic chains.

Determining of the mean-square unperturbed end-to end distance, $\langle r^2 \rangle_0$, use the classic rotational isomeric state model for the partition of configurations in chains unperturbed by long-range interactions. The values of $\langle r^2 \rangle_0$ are transformed to the characteristic ratio, Cn,

$$C_n = \frac{\langle r^2 \rangle_0}{nl^2} \tag{2.1}$$

where *n* denotes the number of C-C bonds of length *l*.

Three rotational isomeric states are employed for such internal bond. First- and second-order interactions are employed in the 3 × 3 statistical weight matrices, ***U***. In the description of the chain with *m* and *r* diads (Flory, 1974), the statistical weight matrix for the C^a-C bond is

$$U_p = \begin{bmatrix} 1 & 1 & 1 \\ 1 & 0 & 1 \\ 1 & 1 & 0 \end{bmatrix} \tag{2.2}$$

where C^a denotes the carbon atom bearing a chlorine atom. The matrix for the next bond, which accomplishes the diad, is either ***Um*** or ***Ur***,

$$U_m = \begin{bmatrix} \eta^2\omega_{xx} & \eta & \eta\tau\omega_x \\ \eta & \omega & \tau\omega_x \\ \tau\eta\omega_x & \tau\omega_x & \tau^2\omega\omega_{xx} \end{bmatrix} \tag{2.3}$$

$$U_r = \begin{bmatrix} \eta^2 & \eta\omega_x & \eta\tau\omega_{xx} \\ \eta\omega_x & 1 & \tau\omega \\ \eta\tau\omega_{xx} & \tau\omega & \tau^2{\omega_x}^2 \end{bmatrix} \tag{2.4}$$

depending on whether the *diad* is *m* or *r*. Rows and columns are indexed in the order *t, g+, g-* (Flory, 1974), with columns indexing the states of the present bond and rows indexing the states of its ancestor.

Equitably, the chain can be described along with *d, l* pseudo-asymmetric centers and statistical weight matrices defined by

$$\boldsymbol{U}p = \boldsymbol{Q}\boldsymbol{U}d = \boldsymbol{U}_l\boldsymbol{Q}$$

$$\boldsymbol{U}m = \boldsymbol{U}_{dd}\boldsymbol{Q} = \boldsymbol{Q}\boldsymbol{U}_{ll}$$

$$\boldsymbol{Ur = U_{dl} = QU_{ld}Q}$$

The statistical weights showing in the matrices are for first-order interactions in the t and g+ states (η and τ, respectively) and second-order interactions between two carbon atoms in the backbone, between a carbon atom and a chlorine atom, and between two chlorine atoms (ω, ω_X, and ω_{XX}, respectively).

The geometry and statistical weights are intimately related to those described recently by Smith et al. (Smith, 1995). The bond angles are 112° and 116° for ∠C-C^a-C and ∠C^a-C-C^a, respectively. Within a *dd* (*ll*) *diad*, the torsion angles are -178° (178°), 61° (60°), -60° (-61°) at the C^a-C bond and 178° (-178°), 60° (61°), -61° (-60°) at the C-C^a bond, both given in the sequence *t*, *g*+, *g*-. Within a *dl* (*ld*) diad, these torsion angles are 175° (-175°), 66° (62°), -62° (-66°) at the C^a-C bond and at the C-C^a bond. The statistical weights were calculated as Boltzmann factors, using the energies E_η = -0.9, E_τ = -0.5, E_ω = 3.0, $E\omega_X$ = 2.3, and $E\omega_{XX}$ = 4.0, all expressed in kcal/mol. The temperature was 373 K. Calculations of C_n were performed using the program V2.RIS, for which the FORTRAN source code (Mattice, 1994).

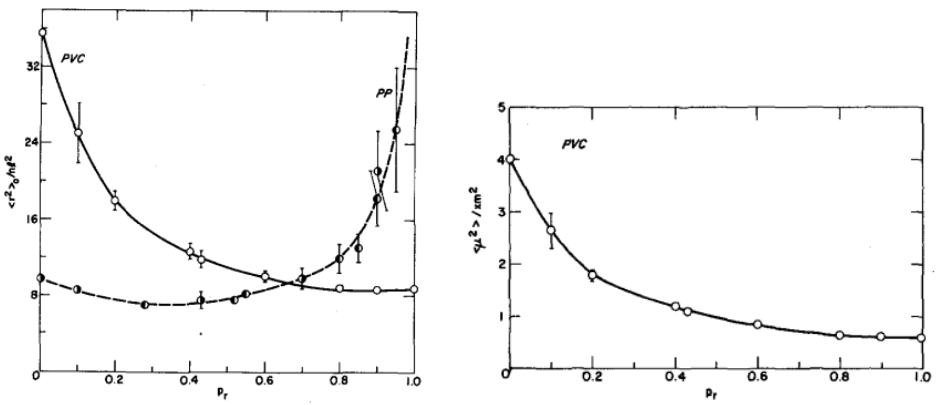

Figure 2.1 The characteristic ratios, (C_n = $\langle r^2\rangle_0/nl^2$), and dipole moment ratio, (C_m = $\langle m^2\rangle_0/nm^2$), for PVC chains with Bernoullian tacticity and a probability for a repeating diad P_r (equivalent to the probability of *meso* diad).

2.1.2 Rotational isomeric state (RIS) model of PVF

For example, the RIS model for vinyl–[CH_2-CH(X)]$_n$- chains, where all bonds have 3-fold symmetry of their torsion potential with the nearest neighbor determined by a statistical weight matrix for consecutive C-C$^{\alpha}$ and C$^{\alpha}$-C bonds. With the stereochemistry of pseudo-asymmetric centers, the statistical weight matrices for the C$^{\alpha}$ –C bond is

$$U_d = \begin{bmatrix} \eta & 1 & \tau \\ \eta & 1 & \tau\omega \\ \eta & \omega & \tau \end{bmatrix} \tag{2.5}$$

when the fluorine atom is attached to C$^{\alpha}$ with *d* configuration.

The statistical weight matrices for the C–C$^{\alpha}$ bonds depend on two successive pseudo-asymmetric centers as

$$U_{dd} = \begin{bmatrix} \eta\omega_{xx} & \tau\omega_x & 1 \\ \eta & \tau\omega_x & \omega \\ \eta\omega_x & \tau\omega\omega_{xx} & \omega_x \end{bmatrix} \tag{2.6}$$

$$U_{dl} = \begin{bmatrix} \eta & \omega_x & \tau\omega_{xx} \\ \eta\omega_x & 1 & \tau\omega \\ \eta\omega_{xx} & \omega & \tau\omega_x^2 \end{bmatrix} \tag{2.7}$$

For an *l* configuration, the statistical weight matrices for these bonds can be found by

$$U_l = QU_dQ,\ U_{ll} = QU_{dd}Q \text{ and } U_{ld} = QU_{dl}Q \tag{2.8}$$

where $Q = \begin{bmatrix} 1 & 0 & 0 \\ 0 & 0 & 1 \\ 0 & 1 & 0 \end{bmatrix}$

In these statistical weight matrices, the rows and columns refer to the conformation of bonds *i*-1 and *i*, respectively. Three conformational states are *t*, *g*+, and *g*-, ordered in the matrices. The reference state corresponds to the conformation with CH...CH_3 arrangement. The first-order energy E_η is defined for the bond conformation with CH...F interaction but no CH...CH_3 interaction, while a conformation resulting in both a CH...F and CH...CH_3 interaction is another first-order energy E_τ. In addition, E_ω, E_{ω_x} and $E_{\omega_{xx}}$ are the energy of the second-order CH_3...CH_3,

CH_3... F and F... F pentane-type interaction, respectively. For PVF, E_{wp} is the energy for F...F interaction when the chain has W conformation.

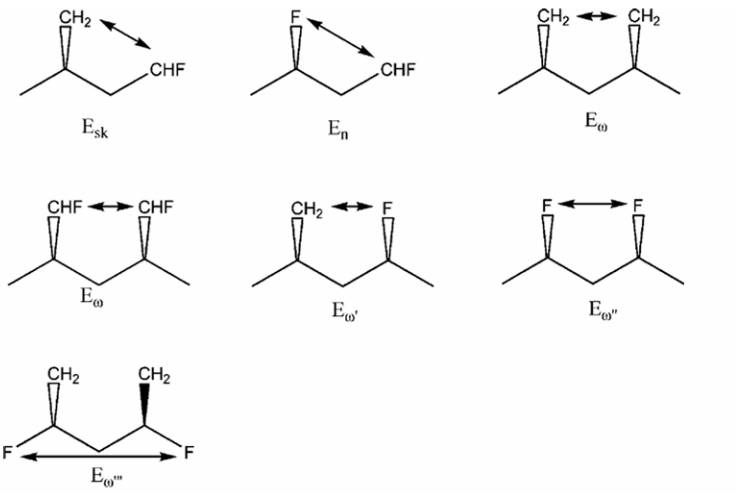

Figure 2.2 Characteristic interactions of PVF.

The main purpose of this work is to examine structures, dynamics and material properties of amorphous PVC and PVF at the bulk density by multiscale simulation technique. In general, this method consists of four steps: (i) determination for statistical weights for conformational statistics of PVC and PVF chains based on quantum chemistry calculation (ii) mapping of an atomistic PVC or PVF chains to the coarse-grained representation on the *2nnd* lattice, (iii) performing MC simulations on the *2nnd* lattice, and (iv) reverse mapping of selected snapshots from the *2nnd* lattice back to fully atomistic models. Many examples of this simulation have been performed during many years ago inclusive homogeneous polymers and their mixtures such as polyethylene, poly(ethylene oxide), polypropylene, polystyrene and polyvinyl alcohol (Cho, 1997; Doruker, 1997 and 1999; Haliloglu, 1998; Clancy, 2000; Jang, 2000; Vao-soongnern, 2000, 2001, 2004, 2006, 2010 and 2014; Akten, 2001; Xu, 2002 and 2003; Choi, 2004; Rane, 2004 and 2005; Dionne, 2005 and 2006; De la Rosa, 2002). In this work, we employ the coarse-grained model to investigate the structures and dynamics of bulk *a*PVC and *a*PVF melts. In addition, the fully atomistic models can be obtained from the reverse-mapping procedure to determine their material properties. The main focus is to validate the simulation method for the specific polymer with a comparison

to the prediction from theory and experimental results. This investigation is an extension of our recent published work on PVA and PS (Wichai, 2021; Kusinram, 2022).

2.2 Monte Carlo simulation : Effect of chain stiffness on the free surface of polymers

Most of these past studies have mostly limited to the surfaces of polymers with relatively flexible chains. It is of interest to see how the surface properties can be changed if polymer chains become more flexible or stiffer as chemical modification of polymers can give new molecules with different degrees of chain stiffness. For example, perfluoro-polymers usually exhibit stiffer chains compared to analog molecules such as polytetrafluoroethylene -(CF_2CF_2)- vs polyethylene -(CH_2CH_2)- (Smith, 1994).

The chain stiffness arising from barriers to bond rotation and structural constraints are closely related to the macroscopic properties of polymers. For computer simulation, the degree of local flexibility can be adjusted by manipulating the intramolecular energetics can affect the molecular and structural properties of polymer surfaces. In principle, the simulation of fully atomistic models should provide the most detailed information as one can consider the specific chemistry of polymer chains. Because of their long time and large length scales, polymer simulations at the atomistic level are normally restricted to rather small molecules with some degree of chain flexibility. Thus, one might question whether atomistic simulation to study polymer surfaces with different degrees of chain stiffness could be done properly. Sufficient equilibration of polymer systems should be confidentially ensured, for instance, the chain end-to-end vector of individual polymers should be fully uncorrelated with their initial orientation, and the mean square displacements for polymer chains should be larger than molecular dimension (Mansfield, 1990; Misra, 1995).

By resorting to coarse-grained (CG) models, the efficacy of polymer simulation can be improved. One approach is Monte Carlo (MC) simulations of CG models on the *2nnd* lattice developed to investigate the free surface of polyethylene (PE) melts with different geometric confinements (Doruker, 1998; Baschnagel, 2000; Vao-soongnern,

2000 and 2001). The energetics of this simulation method are composed of the rotational isomeric state (RIS) model (Flory, 1969; Mattice, 1994) and the Lennard–Jones (LJ) energy function to describe the intra- and intermolecular interactions of polymer chains, respectively. Free surface models of PE melt (108 PE chains with the degree of polymerization = 50) can be effectively created and equilibrated by this MC simulation (Doruker, 1998). Subsequently, molecular, structural, and dynamic characteristics of the free surface of PE melts can be determined from these CG models. It is possible to extend this simulation method to incorporate the chain stiffness on polymer surfaces. The concept of the "*polyethylene-like*" model was recently proposed so that the effect of chain stiffness can be determined systematically on the free surfaces of polymer melts. Note that this MC method can be extended to generate the atomistic models as reported recently (Vao-soongnern, 2014; Wichai, 2021; Kusinram, 2022).

In this work, structural and molecular properties of the free surface of the polymer melt with different degrees of chain stiffness are investigated using *polyethylene-like* models. First, the important feature of modeling polymers with different chain stiffness is presented. The simulation method and the technique to generate polymer surfaces are described, followed by the results, discussion, and conclusion.

2.3 The effect of intermolecular interaction on polymer crystallization

Polymer crystallization is a relatively slow process, especially near the melting point, and often occurs by the kinetic-controlled mechanisms far from thermodynamic equilibrium (Yamamoto, 2009). Molecular simulations can be applied to rigorously monitor molecular mechanisms in these non-equilibrium states. Nevertheless, due to the very slow dynamics, computer simulation has long been beyond the scope of fully atomistic models to investigate polymer crystallization (Hu, 2005; Muthukumar, 2005; Luo, 2009). With new developments in calculation algorithms and the increasing power of computational resources, computer simulations can also be performed to examine the assumptions of theoretical models, predict experimental results, and suggest underlying microscopic details. Computer simulations have been used to understand

molecules in terms of issues including crystal formation, crystal-amorphous interfaces, temperature protocols, molecular weights, and bond stiffness (Ergoz, 1972; Mavrantza, 2001; Lavine, 2003; Gee, 2006; Koyama, 2008; Luo, 2011, 2013 and 2016; Piorkowska, 2013; Yi, 2013; Yamamoto, 2005 and 2014; Jabbari-Farouji, 2015; Nguyen, 2015; Ramos, 2015). Despite more advancements in computer hardware, realistic simulations of physical systems at the atomic scale are still difficult in practice. To solve this problem, molecular simulations of CG models have been developed to investigate polymer crystallization to cover a wider range of length and time scales (Fujiwara, 1997; Meyer, 2001 and 2002; Reith, 2001). For example, crystallization in dilute solution for polymers with varying chain rigidity, which has a strong influence on the folding kinetics of polymers in the crystal structure, has been studied by MC simulations (Chen, 1998).

The role of interaction potential energies or "*forcefield*" (FFs) for molecular models on the crystallization of PE melts has been studied by MD simulation (Yamamoto, 2013; Anwar, 2015; Luo, 2017; Xiao, 2017; Verho, 2018). It was found that FF parameters greatly influence the PE crystal growth rate, and several FF parameters have been proposed, such as the united atom (UA) model, which is widely used to study PE crystallization (Ramos, 2015). There are several reports on the polymer crystallization of a single long PE chain upon cooling from the melting temperature, (Kavassalis, 1993; Sundararajan, 1995; Fujiwara, 2001; Yamamoto, 2013). The pioneering investigation of these works using DREIDING UA FF (Mayo, 1990) was successful as it can promote the *trans* state in PE crystallization. For the original UA model with DREIDING FF, the LJ parameters of the CH_2 beads were treated by the averaged values from CH_4 and C parameters. However, it was reported a problem of too large fraction of the *trans* state with DREIDING-UA FF (Jabbari-Farouji, 2015). Several FF parameters were then proposed to improve the crystallization of PE by MD simulations of UA models, mostly for short alkanes (Rigby, 1987; Esselink, 1994; Paul, 1995; Harmandaris, 1998; Mavrantzas, 1998; Fujiwara, 1998 and 1999; Takeuchi, 1998; Koyama, 2002 and 2003; Waheed, 2002 and 2005; Ko, 2004; Yi, 2009 and 2011; Nicholson, 2016; Welch, 2017). In addition, simulations were also compared between UA and atomistic (AA) models to determine the chain folding of a single PE molecule (Li, 2010). The fraction of the *trans* state in PE crystal with the AA model was lower than in the UA model.

The folding behavior was impossible for UA FFs with $\sigma_{LJ} > \sigma$ (LJ diameter of CH_2) because the probability distribution of the torsion angle has no *gauche* minima. In addition, the atomistic united-atom representation of PE which was demonstrated, through Monte Carlo simulations, to provide very accurate predictions for the volumetric and size properties of PE chains under a wide variety of conditions, including temperature and average molecular weight (Karayiannis, 2002; Foteinopoulou, 2009; Anogiannakis, 2012).

Another lattice MC simulation of CG models has been proposed to investigate polymer crystallization from the melts (Baschnagel, 2000). Chains are represented by the rotational isomeric state (RIS) model to describe the short-range intramolecular interaction and the LJ potential energy to treat the long-range intermolecular interactions between CG beads (monomer units), respectively. This lattice-based MC method can be applied to simulate polymers with chemical details and the CG model can be reverse-mapped back to the fully atomistic structure (Wichai, 2021; Kusinram, 2022). Previously, this simulation technique has been employed to investigate PE crystallization in different situations such as nanofiber (Xu, 2002), nanoparticle (Vao-soongnern, 2004), cyclic vs linear chains (Jamornsuriya, 2022), mixed molecular weights (Vao-soongnern, 2023), and polymers with varied degrees of the chain stiffness (Sirirak, 2023). Generally, the long-range interaction among non-bonded units is obtained from the LJ interaction among ethylene units since each CG bead represents a repeating (CH_2CH_2) unit of PE. Because the LJ parameters for -CH_2CH_2- as a portion of a long chain are unknown, it is suggested that the non-bonded LJ interaction parameters should be within the range of CH_2CH_2 but should not exceed those values for CH_3CH_3. The LJ parameters determined from the viscosity data for CH_2CH_2/CH_3CH_3 molecules are σ = 0.42/0.44 nm and ε/k = 205/230 K (Poling, 2002). Typically, two sets of LJ parameters were proposed by comparing bulk properties obtained from simulation to experimental data such as the cohesive energy *i.e*. set I (σ = 0.44 nm and ε/k = 185 K) and set II: (σ = 0.42 nm and ε/k = 205 K), used successfully to investigate structures and dynamics in the past simulations of PE melts (Cho, 1997).

Nevertheless, it was found that only the parameter set I (σ = 0.44 nm and ε/k = 185 K) can be applied successfully to observe the crystallization upon cooling from

the melts while simulations with parameter set II give quite disordered structures with a low degree of chain orientation (a slightly different parameter set, σ = 0.42 nm and ε/k = 185 K, was also applied and the structure formation can be observed clearly for PE crystallization). As the main difference in the LJ parameters between sets I and II is from the potential well depth (ε), the sensitivity of the intermolecular interaction on polymer crystallization from the molten sate is explored here by MC simulation of CG *PE-like* models *i.e.* the same bead dimension (σ = 0.44 nm) but different potential well depth (ε/k = 125-205 K) for more repulsive and more attractive interactions compared to the normal PE chains.

2.4 Molecular dynamics (MD) simulation of detailed structures and ion transportation of polymerized ionic liquid/ionic liquid blends

PILs include charged groups with an ionic liquid structure in the main and/or side chains, which is weakly coordinated with opposite charges counterions. One of the major challenges for the application of polymers such as PIL as electrolytes is to create highly conductive while maintaining strong mechanical properties (Shaplov, 2018; Rochow, 2020; Yoshizawa-Fujita, 2021). Consequently, understanding the structures and dynamics of PILs and counter ions with their correlations is necessary in designing PIL-based materials with better performance. We employed molecular dynamics simulations to carry out ion mobilities and the molecular mechanisms of transport in blends of [poly(1-butyl-3-vinylimidazolium bis(trifluoromethanesulfonyl)imide): Pbvim-TFSI] electrolytes with [1-butyl-3-methylimidazolium bis(trifluoromethanesulfonyl)imide : Bmim-TFSI] ionic liquids.

2.4.1 Ionic conductivity in Experiment

The classical Nernst–Einstein (NE) equation relates the ionic conductivity to ion diffusion, D_i (Kremer, 2003):

$$\sigma = \frac{1}{kT}\sum_i n_i {q_i}^2 D_i \tag{2.9}$$

Where, n_i is the concentration and q_i is charge, of the free ions participation to conductivity.

In a clarified random walk estimation, indicating that the diffusion coefficient can be displayed over the average jump length λ_i and the rate of ion jumps $1/\tau_i$. It is

assumed that the ion diffusion reaches the Fickian regime after the first jump. We emphasize that $1/\tau_i$ is the obvious ion jump rate (Sangoro, 2011).

$$D_i \sim \lambda_i^2 \,/\, (6\tau_i) \tag{2.10}$$

2.4.1.1 Mechanisms of ionic conductivity in polymer electrolytes.

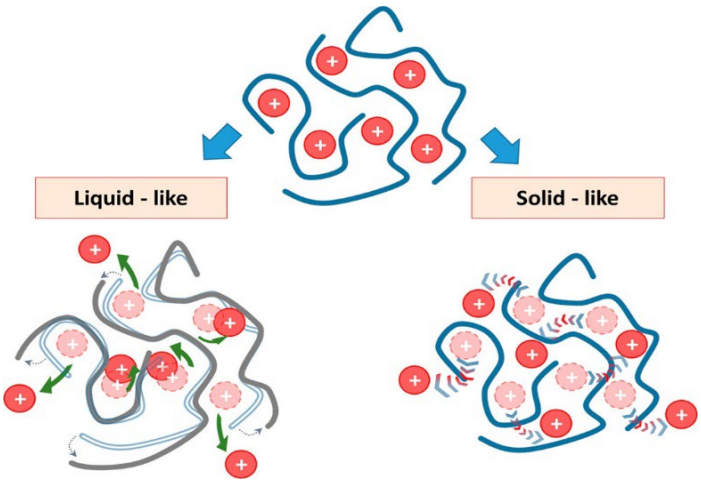

Figure 2.3 Schematic presentation of two possible mechanisms of ion transport in polymers: the liquid-like (lower left) requires the motion of the polymer segment and depends on the rate of segmental relaxation, whereas the solid-like (lower right) is based on ion jumps over an energy barrier in the frozen (on the time scale of ion jumps) polymer matrix (Bocharova, 2020).

2.4.1.1.1 Liquid-like Mechanism:

The first mechanism always reveals a Vogel–Fulcher–Tammann (VFT) temperature differentiation, following the temperature subordination of the structural relaxation and viscosity (Choi, 2014; Zhang, 2017; Kisliuk, 2019; Yao, 2019; Bocharova, 2020):

$$\sigma_i = \frac{A}{T} exp[-\frac{E_a}{kT}] \tag{2.11}$$

Where, *A* refers to the pre-exponential factor, k is the rate constant, and E_a is the activation energy for conductivity.

Ion conductivity follows the VFT-like behavior at T >T_g (Choi, 2014). Any interpolation of the polymers, and gathering of ions, lead the way an important improvement in T_g and decelerating of segmentary relaxation at ambient temperature.

As a consequence, using the liquid-like mechanism has fundamental restriction and unfeasible to produce the desired level of ionic conductivity in dry polymer electrolytes at ambient temperature. Powerful acceleration of polymer segmental dynamics can be brought to fruition by adding small molecular plasticizers.

2.4.1.1.2 Solid -like Mechanism:

This mechanism illustrates a vigorous decoupling of ion diffusion from structural relaxation in superionic systems. In this case, ion diffusion occurs in a principally frozen structure through the solid-like mechanism. Generally, ion jump motion and polymer chain relaxation and/or segmental motion together affect conductivity, so the ionic conductivity in SPEs is usually modeled by the VTF equations with non-linear relationship (Choi, 2014; Zhang, 2017; Kisliuk, 2019; Yao, 2019; Bocharova, 2020):

$$\sigma_i = \sigma_0 T^{-\frac{1}{2}} exp[-\frac{B}{T-T_0}] \quad (2.12)$$

where B is the pseudo-activation energy, σ_0 is the pre-exponential factor, and T_0 is the reference temperature. So, polymer electrolytes show an Arrhenius temperature dependence of conductivity at $T < T_g$ (Choi, 2014).

2.4.2 The charge screening on the viscoelastic properties and the conformation of polymerized ionic liquids (PILs) in ionic liquid (IL) solutions

Matsumuto et al. (Matsumoto, 2019), they conduct detailed rheological characterization of a model system containing a PIL [PC_4-TFSI: poly(1-butyl-3-vinylimidazolium bis(trifluoromethanesulfonyl)imide)] in a mixture of a salt-free solvent (DMF: dimethylformamide) and an ILs [Bmim-TFSI : 1-butyl-3-methylimidazolium bis(trifluoromethanesulfonyl)imide] solution, with low to high IL concentrations, while spanning dilute and semidilute polymer regimes.

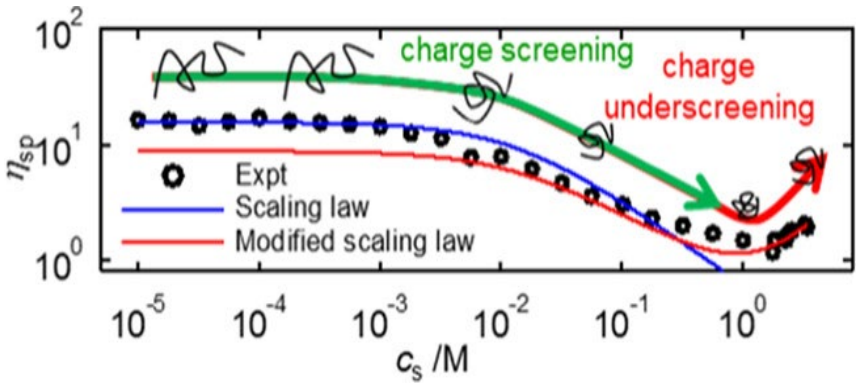

Figure 2.4 Specific viscosity as a function of the concentration of Bmim-TFSI for PC_4-TFSI solutions at cp = 4.0 × 10^{-2} M. The values of η_{sp} via a bulk shear rheometer (ARES-G2; open circles), a microfluidic-based rheometer (m-VROC; open diamonds), and a gravity-driven capillary viscometer (Ubbelohde; filled circles) are compared. Blue solid and red dashed curves represent the scaling prediction of η_{sp} for semidilute unentangled (SUF) and DF* solutions, respectively.

They then studied the four different polymer concentrations ranging from c_p = 8.0 × 10^{-4} to 4.0 × 10^{-2} M, with the ionic liquid concentration 0 M ≤ c_s ≤ 3.42 M. Specifically we identified three regions: (i) at low c_s, η_{sp} and λ,remained constant with increasing c_s; (ii) at an intermediate c_s, η_{sp} and λ, decreased with increasing c_s; (iii) at sufficiently high c_s, η_{sp} and λ, increased with increasing c_s. Regions (i) and (ii) were well described by the scaling laws of Dobrynin et al. (Dobrynin, 1995). for ordinary polyelectrolytes in a good solvent.

2.4.3 Molecular Dynamics (MD) Simulation of polymerized ionic liquids

Molecular dynamics (MD) simulation is the force field-constructed procession to investigate the trajectory of atomic movement followed by Newtonian equation of motion. The average values can be assessed using the statistical mechanic principles to link the microscopic trajectories to predict static and dynamic properties at the macroscopic level. The calculation for bond stretching and bending motion are quite taking very long time, as they have large force constants. Because the performance of current computer technology is not powerful enough, these two terms are generally fixed. Consequently, the properties of polymer usually depend on the other energetic terms: torsional energy and non-bond energies, as shown by:

$$E = E_{covalent} + E_{non-bond} \quad (2.13)$$

Where $$E_{covalent} = E_{bond} + E_{angle} + E_{torsion} \quad (2.14)$$

$$E_{non-bond} = E_{electrostatic} + E_{van\ der\ waals} \quad (2.15)$$

Molecular dynamic (MD) simulation is based on the statistical mechanic formalism that links the macroscopic properties of the bulk materials to their microscopic parameters. MD simulation generates a series of configurations as a function of "time". Each of simulated system consists of the kinetic energy, potential energy, thermodynamic properties, and the structure at a particular state or ensemble. This is because MD can change each configuration both the structure and momentum under thermodynamic equilibrium. If one gets enough number of these "snapshots", one can evaluate the macroscopic properties of the system of interest.

The main trust of MD simulation is to solve the Newtonian equation of motion for the system composed of N atoms that interact among themselves through the potential function called "force field". The interacting force (F_i) on each particle which is a function of time can be obtained from the derivative of the potential function (force field) to the position of this particle as the equation

$$F_{r_i} = -\frac{\partial U}{\partial r_i} \quad (2.16)$$

where F_{r_i} is the force acting on the ith particle, U is the function of potential energy and r_i is the position of the *i*th particle.

The position and velocity of the particle at the next time step can be evaluated by extending the current position and velocity of the particle using Newtonian's equation of motion. This equation is originally written as $F_i = m_i a_i$ where the accelerator (a_i) for each particle can be calculated from the reaction force (F_i) and the mass of the particle according to the equation:

$$a_i = \frac{F_i}{m_i} \rightarrow \frac{d^2 r_i}{dt^2} = \frac{F_i}{m_i} \quad (2.17)$$

The solution of this second-order differential equation with time ($\frac{d^2 r_i}{dt^2}$) can be obtained by the integration of each particle throughout the time span as

$$\frac{\partial r_i}{\partial t} = \left(\frac{F_i}{m_i}\right) t + c_i \quad (2.18)$$

For the boundary condition, at t = 0, the initial velocity (u_i) will be a constant value of c_i and the velocity at time t is $\frac{\partial r_i}{\partial t} = a_i t + u_i$. If *a* is also constant, one can further integrate to result in the following relation

$$S_i = u_i t = \frac{1}{2} a_i t^2 + c_2 \tag{2.19}$$

as where c_2 is another constant that is related to the position at the present time. Hence, all the changes can be calculated from the initial velocity u_i and accelerator $a_i \frac{F_i}{m_i}$.

The format of the above equation is in accord with the approximation using Taylor's series expansion up to the second degree as the relation:

$$x(t + \Delta t) = x(t) + \left(\frac{dx}{dt}\right)\Delta t + \left(\frac{d^2x}{dt^2}\right)\frac{\Delta t^2}{2} + \ldots \tag{2.20}$$

From this equation, if one knows the position (first term), the velocity (second term) and the accelerator (third term) at the time *t*, one can calculate the position and velocity for the time t+ Δt (in practice, the time step Δt is the time interval at which the particles change their position. Usually, we set Δt in the range of femtosecond). There are many numerical algorithms used for solving this integration function of motion such as Verlet, Leap-frog and Beeman. All of them are similar as they consist of looping and changing coordinate for every atom in the system. A set of atomic configurations for the MD run can be averaged in an appropriate ensemble to result in some parameters of interest such as the average distance between atom pair and the coordinations number of the reference atom.

2.4.4 Molecular Dynamics (MD) Simulation of Ionic conductivity

In addition, the ionic conductivity can be determined microscopically from the movement of ions obtained from the MD trajectory. The diffusion coefficient can be calculated as an ensemble average of the center-of-mass vector of a molecule or ion at the time $t, R(t)$, $6Dt = \langle |R(t) - R(0)|^2 \rangle$. An alternative way is to use the center-of-mass velocity autocorrelation function of each species. $3D = \int_0^\infty \langle v(t)v(0) \rangle dt$. The conductivity (at zero frequency) can be equated to $3Vk_BT\lambda = \int_0^\infty \langle j(t)j(0) \rangle dt$ Here, V is the volume, k_B is Boltzman constant, T is temperature. The flux of charge is given

by $j(t) = e\sum_{ions} q_i v_i(t)$ where e is the elementary charge and q_i is the formal charge of **ion** i. The Einstein equation equivalent to Kubo equation can also show by

$$6tVk_BT\lambda = e^2\left\langle \sum_i \sum_j q_i q_j \times [R_i(t) - R_i(0)]\left[R_j(t) - R_j(0)\right]\right\rangle \quad (2.21)$$

The cross term (i≠j) in this equation is for the correlation between the diffusion of two different ions.

In molecular dynamics simulations, this is suitable to describe the upon equation in the format of an impartial Einstein relation:

$$\sigma = \lim_{t\to\infty} \frac{e^2}{6tVk_BT}\left\langle \sum_i \sum_j q_i q_j \times [R_i(t) - R_i(0)]\left[R_j(t) - R_j(0)\right]\right\rangle \quad (2.22)$$

As discussed by McDaniel et al. (McDaniel, 2018). The conductivity can be split into five components: $\sigma = \sigma_+^s + \sigma_-^s + \sigma_+^d + \sigma_-^d + \sigma_{+,-}^d$ where the cation– self $(\sigma_+^s = q_+^2 D_+ N_+/(Vk_BT))$, anion– self $(\sigma_-^s = q_-^2 D_- N_-/(Vk_BT))$, cation-distinct (σ_+^d), anion-distinct (σ_-^d), and cation/anion-distinct $(\sigma_{+,-}^d)$ conductivities all contribute to the total conductivity.

If the ions all move independently, then the cross-terms are zero, and the Nernst–Einstein relationship applies (Demir, 2020):

$$\sigma_{NE} = \frac{1}{Vk_BT}\left(q_+^2 D_+ N_+ + q_-^2 D_- N_-\right) \quad (2.23)$$

Where D_+ (D_-) and N_+ (N_-) are the diffusion coefficient and the number of cations (anions), respectively.

From the cross-correlation term is small and hence may be neglected. As a result, we arrive at a modified Nernst-Einstein equation based exclusively on the free ions:

$$\sigma_{NE,\text{modified}} = \frac{1}{Vk_BT}\left(q_+^2 D_+ N_+ p_+ + q_-^2 D_- N_- p_-\right) \quad (2.24)$$

Where p_+ and p_- are fractions of cations and anions in the free state (Feng, 2019).

2.4.5 Ion Transport Mechanisms

Mixtures of polyILs with pure ILs compose a stimulating level matter with potential for desired property characteristics. Such materials share features in common with plasticizer-doped polymer electrolytes (Abraham, 1997; Song, 1999; Scott, 2002), wherein the additive (in this case, pure ILs) can serve as a means to accelerate the

polymer dynamics and whereupon enrich the conductivity. Nevertheless, when compared with traditional plasticizers, ionic liquid additives can also encourage mobile ions and increase the overall conductivity of the electrolyte. Furthermore, as a resultant of the decoupling phenomena considered above, such blends may also offer a wider parameter space to override the conductivity–mechanical strength trade-off.

Santosh and Venkat (Mogurampelly, 2018). They used atomistic molecular dynamics simulations to study ion mobilities and the molecular mechanisms of transport in blends of poly(1-butyl-3-vinylimidazolium hexafluorophosphate) electrolytes with 1-butyl-3-methyl-imidazolium hexafluorophosphate ionic liquids. At all temperatures, the diffusion coefficients of both were examined both $BMIM^+$ and $PF6^-$ ions diminish monotonically with expanding polyIL wt %. Such outcomes confirm the speculation underlying their research and illustrates that blending polyILs with pure ILs can actually bring about an elevation in the ion mobilities relative to polyILs. And between the various blends the decoupling consequence is most dominant in comparing pure ILs with the different blend complements and that the dissimilarity in the ion mobilities turns into less essential when comparing nonidentical blend ratios. From the simulation results for the true conductivity and the NE values as a function of the polyIL wt% and T/T_g. Interestingly, it is seen that while both the NE and the direct conductivities exhibit a "decoupling" from T/T_g, the degree of such effects becomes significantly reduced when compared to the ion mobilities. After that the ion transport mechanisms within the polyIL–IL blends were explored to offer molecular type enlightenments. Their outcomes propose that the intrachain interaction transport mechanism implying ion hopping along polymer chains is outstanding of all the transport events.

Xubo et al. (Luo, 2021). They study the ion-transport mechanism in poly(ethyl vinyl imidazolium) with different anions: Br^-, BF_4^-, PF_6^-, and Tf_2N^- by MD simulations.

These results indicate that anion diffusivity (D_A) calculated with the Einstein relation from mean square displacements (MSDs) of the simulation trajectories, Br^- has much lower diffusivity than the other anions, while the other three anions do not exhibit large differences at any of the temperatures. Generally, it is observed that $Tf_2N^- > BF_4^- > PF_6^- > Br^-$. For the distinct part of the van Hove function, $G_d(r,t)$, show

that the nontrivial peaks at r = 0 specify correlated motion, where it is possible for an anion to occupy the position of another anion as a replacement. The much higher peaks at r = 0 for Br^-, BF_4^-, and PF_6^- indicate the precise replacement, while the lower peaks for Tf_2N^- are probably due to its flexibility as the center of mass of Tf_2N^- has more freedom to fluctuate. And length of stringlike motion, indicate that they do not observe significantly more immobile ions in the Tf_2N^- system, the shorter strings are not due to less mobility. It can be due to its larger size and multiple conformations. It might be possible that poly(C_2Im) Tf_2N is more flexible such that the hopping of Tf_2N^- at $t = t^*$ may not exactly locate the position of the replaced ion at t = 0.